early stages of x irradiation there is a low density of trapped electrons, hence a ferromagnetic state exists. As the x-ray bombardment is continued the concentration of trapped electrons increases and there are very few unpaired electrons resulting in the destruction of the ferromagnetic state.

According to the theory of Bloch[7] the ferromagnetic state exists for low concentrations of electrons because the electrons have parallel spins and stay far apart in order to keep their Coulomb repulsion reduced as much as possible. This is a direct consequence of the Pauli exclusion principle.

It has also been observed that if the crystals are permitted to age approximately one month with respect to the last period of x irradiation, the magnetic moment returns the value it had prior to any x irradiation, indicating that the trapped electrons are only stable in a specified concentration per dislocation given by the preirradiation value. High concentrations may slowly evaporate away at room temperature if the trapping depth is small.

The experimental evidence presented in this paper would seem to rule out the possibility that the observed ferromagnetism arises from nickel or iron precipitates in the crystal. It does however support the idea that the ferromagnetic effect arises from the $10^{14}$ electrons trapped at dislocations in these crystals.

[7] F. Bloch, Z. Physik **57**, 545 (1929).

## ACKNOWLEDGMENTS

The authors acknowledge with thanks discussions and suggestions by Professor C. F. Squire and Professor J. L. Gammel. For fellowships held during the course of this research one of the authors (E.J.S.) wishes to thank NASA and the other (D.A.A.) wishes to thank the National Science Foundation. They also wish to thank the Robert A. Welch Foundation for their financial support of this research.

PHYSICAL REVIEW VOLUME 158, NUMBER 2 10 JUNE 1967

# Experimental Determination of the Optical Density of States in Iron*†

ALBERT J. BLODGETT, JR.,‡ AND W. E. SPICER
*Stanford Electronics Laboratories, Stanford University, Stanford, California*

(Received 3 February 1967)

Energy distributions of photoemitted electrons and the spectral distribution of quantum yield from iron ($\phi=4.8$ eV) have been measured to a maximum photon energy of 11.6 eV. These data are presented and interpreted in terms of the electronic structure of iron. No evidence is found in these data consistent with the assumption that conservation of **k** is an important selection rule. Rather, it is found that the data can be interpreted in a consistent manner if the optical transition probability is assumed to depend only on the initial and final densities of states. The results allow determination of the optical density of states in the regions $-6.0\leq(E-E_F)\leq 0$ and $5.5\leq(E-E_F)\leq 11.6$ eV, where $E_F$ is the energy of the Fermi level. Maxima are found in the valence-band optical density of states at 0.35, 2.4, and 5.5 eV below $E_F$. This result is similar to that obtained in nickel, except the lowest-energy peak is not as strong and occurs at a lower energy in iron. The conduction-band optical density of states is approximately constant in the region observed. The iron samples were also coated with approximately one monolayer of cesium to reduce the work function ($\phi=1.55$ eV) and thereby extend the range of measurements. Strong transitions are observed near $\hbar\omega=2$ eV, for which the matrix elements vary markedly with $\hbar\omega$. The results, obtained at higher photon energies, are in reasonable agreement with the noncesiated data and suggest that the conduction-band optical density of states decreases monotonically by a factor of two between 2.5 and 5 eV above $E_F$.

## I. INTRODUCTION

IN an earlier paper,[1] the photoemission data on nickel were presented and analyzed. It was shown that the optical density of states[2,3] of Ni obtained from these data differs markedly from that of Cu and that the two are not simply related via the rigid-band model. In this paper, photoemission studies on iron are reported. Iron was chosen as the second ferromagnetic metal to study because the experimental data from Fe coupled with that from Ni would span the three common ferromagnetic metals—Fe, Co, and Ni. A comparison of the experimentally determined electronic structures of Fe and Ni is of particular interest because of the various theoretical models which have been advanced concerning the electronic structure and ferromagnetism in these two metals.[4]

* Work sponsored by the National Science Foundation, and by the Advanced Research Project Agency, through the Center for Materials Research at Stanford University.

† Based on a thesis submitted by A. J. Blodgett, Jr., IBM Resident Fellow, to Stanford University in partial fulfillment of the requirements of the Ph.D. degree.

‡ Present address: International Business Machines Corporation, Components Division, Hopewell Junction, New York 12533.

[1] A. J. Blodgett, Jr., and W. E. Spicer, Phys. Rev. **146**, 390 (1966).

[2] The densities of state obtained from photoemission and optical measurements are called optical densities of states. See Ref. 3.

[3] W. E. Spicer, Phys. Rev. **154**, 385 (1967).

[4] See, for example, N. Mott, Advan. Phys. **13**, 325 (1964), and references given therein.

In this work, the spectral distribution of the quantum yield (SDQY) and energy distributions of photoemitted electrons [energy distribution curves (EDC's)] have been measured as functions of monochromatic radiation to a maximum photon energy of 11.6 eV. In addition, the reflectance of Fe has been measured at nearly normal incidence in the region $2.0 \leq \hbar\omega \leq 11.8$ eV. Since the methods used in the analysis of the data and most of the experimental techniques and equipment used in this work have been reported previously,[1,5,6] only variations in or additions to these methods are discussed here.

## II. EXPERIMENTAL METHODS

The Fe samples used in the photoemission studies were formed by evaporation from Fe-plated tungsten helixes.[7] Each sample was studied both with and without approximately one monolayer of Cs on its surface. The Cs was used to reduce the work function of the metal and thereby extend the range of measurements.[8] To do this, a sample was prepared and first studied without a Cs monolayer. The tube was then resealed onto the vacuum system and approximately one monolayer of Cs was applied to the surface. The resealing was done by use of a "breakoffski" seal so that the pressure of gases other than Cs was maintained $\leq 10^{-9}$ mm throughout the processing.[7]

Reflectance measurements were made by using a small (1.0×0.5×0.1-in.) slab of high purity (99.999%) Fe. The sample was first polished, etched at room temperature for 10 min in a citric-acid–ammonium-hydroxide solution, and then rinsed with acetone, distilled water, and alcohol before insertion into a low-vacuum ($\approx 3\times 10^4$ mm) measuring chamber. (The etching solution was prepared by dissolving 8 g of citric-acid powder in 100 ml of water, and then adding sufficient $NH_4OH$ to just turn litmus paper blue.) This relatively weak etch cleans the surface without destroying the specular reflectance of the sample.

The chamber used for the reflectivity measurements, designed by R. C. Eden, contains a two-position sample mount and is fitted with a Pyrex light pipe which can monitor either the incident or the reflected beam. The output from the light pipe was measured by a photomultiplier. For ultraviolet measurements, the entrance to the light pipe was coated with sodium salicylate.

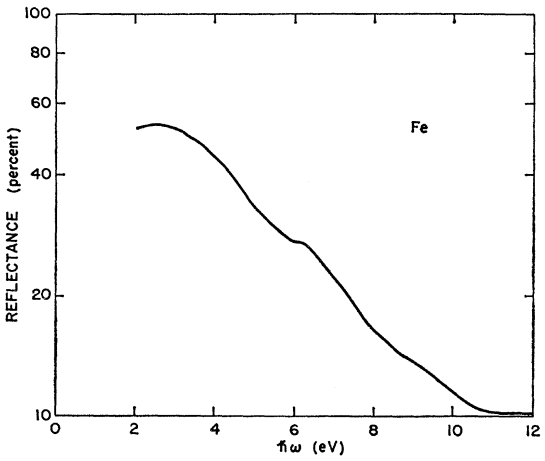


FIG. 1. Reflectance of iron.

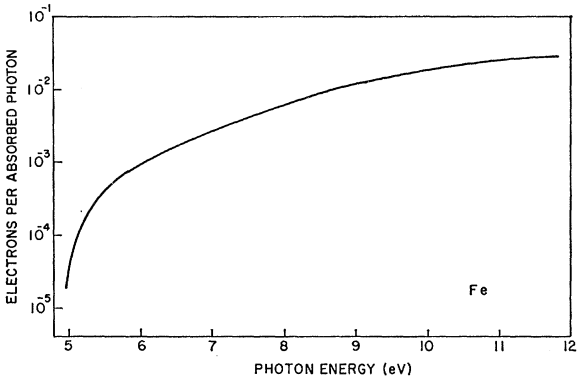


FIG. 2. Quantum yield of iron (without Cs).

## III. REFLECTANCE

The reflectance $R(\omega)$ of Fe was measured because these data are a useful supplement to the photoemission data. First, if the EDC's are to be properly normalized to the quantum yield,[1] the yield must be expressed in terms of electrons emitted per *absorbed* photon; thus, the measured yield (electrons emitted per *incident* photon) must be divided by $[1-R(\omega)]$. Second, the general features of the reflectance can be used to test the results (i.e., the optical density of states and the optical selection rules) deduced from the photoemission data.

The measured reflectance is shown in Fig. 1. These data should be treated with caution since the sample was exposed to air after etching[9] and only low vacuum was used; such procedures can produce surface contamination which can affect the observed reflectance. However, these changes in reflectance usually occur at high photon energies where the reflectance is relatively low.[10] Since an error in $R(\omega)$ does not appreciably change the factor $[1-R(\omega)]$ if $R$ is small, the data

[5] W. E. Spicer and C. N. Berglund, Rev. Sci. Instr. **35**, 1665 (1964).
[6] N. B. Kindig and W. E. Spicer, Rev. Sci. Instr. **36**, 759 (1965).
[7] A. J. Blodgett, Jr., Ph.D. dissertation, Stanford University, 1965 (unpublished).
[8] C. N. Berglund and W. E. Spicer, Phys. Rev. **136**, A1044 (1964).
[9] E. A. Taft and H. R. Philipp, Phys. Rev. **121**, 1100 (1961); H. Ehrenreich and H. R. Philipp, *ibid.* **128**, 1622 (1962).
[10] D. Beaglehole, Proc. Phys. Soc. (London) **85**, 1007 (1965).

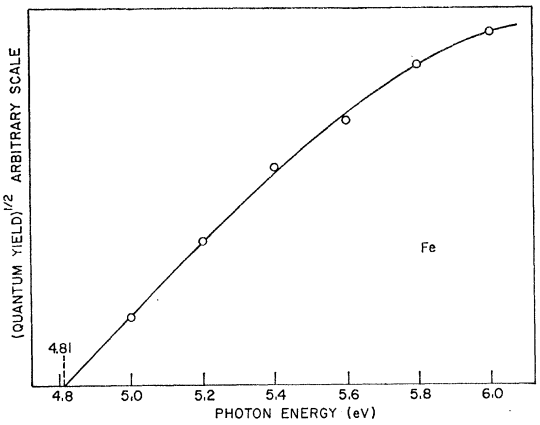


FIG. 3. Evaluation of the work function of iron (without Cs).

presented here are adequate for correcting the yield data.

## IV. PHOTOEMISSION FROM IRON

### A. Quantum Yield

The spectral distribution of the quantum yield of Fe is shown in Fig. 2. This curve has been corrected for the transmission of the LiF window and for the reflectance of Fe. Perhaps the most notable characteristic of the yield curve is the lack of any strong structure.

The square root of the quantum yield was plotted versus photon energy to determine the work function of the sample.[1] This plot (Fig. 3) may be represented near threshold by a straight line which intersects the energy axis at 4.8 eV. This value is used as the work function in Sec. IV.C to determine the energy scale of the density of states with respect to the Fermi level.

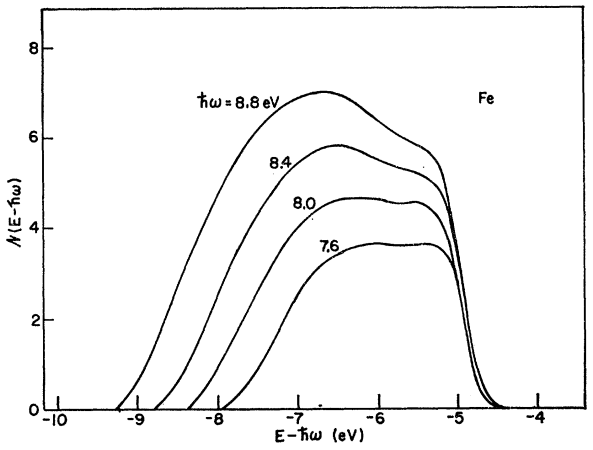


FIG. 4. Energy distributions of photoemitted electrons from iron (without Cs), plotted versus $E-\hbar\omega$, for $\hbar\omega\leq 8.8$ eV.

It is in reasonable agreement with published values[11] of 4.7 eV.

### B. Energy Distribution Curves

Energy distributions of the photoemitted electrons from Fe are shown in Figs. 4–6. These curves have been normalized to the quantum yield (i.e., the area under each EDC has been made proportional to the yield at the corresponding $\hbar\omega$) and have been plotted versus $(E-\hbar\omega)$ to reference the photoemitted electrons to their initial state.[1] The kinetic energy with which the electrons are emitted is represented by $E$. In the $(E-\hbar\omega)$ plots the zero of energy is taken at the vacuum level.

The behavior of the EDC of Fe is quite similar to that observed in Ni.[1] First, the structure above the threshold region does not vary appreciably as the

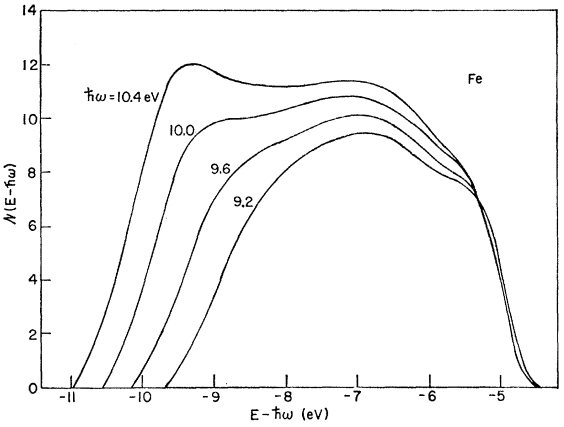


FIG. 5. Energy distributions of photoemitted electrons from iron (without Cs), plotted versus $E-\hbar\omega$, for $9.2\leq\hbar\omega\leq 10.4$ eV.

photon energy is increased from 7.6 to 11.6 eV.[12] This suggests that conservation of $\mathbf{k}$ is not an important selection rule for the corresponding optical transition and that the momentum matrix elements are approximately constant in this range of photon energy.[1,7] Second, the structure in Figs. 4–6 maintains approximately a constant position in energy on an $(E-\hbar\omega)$ plot. This indicates that the structure to the first approximation corresponds to the valence-band optical density of states and that the conduction-band optical density of states is approximately constant in the region of measurement.[1,7] In particular, structure appears at $(E-\hbar\omega)$ values of approximately $-5$ and $-7$ eV. A third peak appears at low energy for $\hbar\omega\geq 10$ eV. It is not clear by visual inspection of these data whether

[11] V. R. Suhrman and G. Wedler, Z. Angew. Phys. **14**, 70 (1960).

[12] The amplitudes of the normalized EDC's in Fig. 4 do not superimpose. This is probably due to an error in the measurement of the quantum yield. Since the same discrepancy appears in the same range of photon energy in the Ni data, the error is likely in the calibration of the light source.

this peak has been completely uncovered at the maximum photon energy (11.6 eV). However, this can be determined by detailed analysis of the data (see below). The structure lying at higher energies becomes increasingly blurred with increasing photon energies. This is believed to be due to the effects of increased electron-electron scattering.[13]

### C. Derived Optical Density of States

In this section, the optical density of states in Fe is derived from the EDC's by use of a model which assumes that the optical transition probability depends only on the initial and final densities of states.[1] The optical density of states so determined is then used to calculate EDC's over a large range of $\hbar\omega$ to demonstrate consistency between the data and the model used in the analysis.

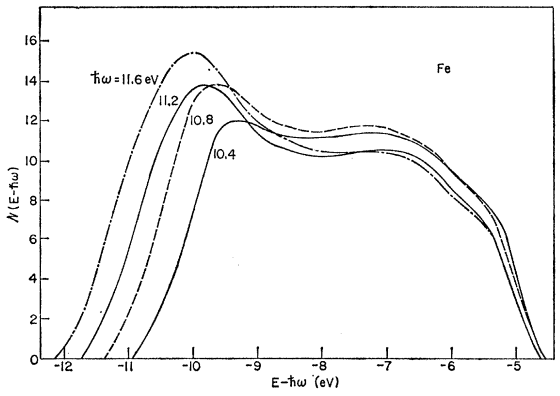


FIG. 6. Energy distributions of photoemitted electrons from iron (without Cs), plotted versus $E-\hbar\omega$, for $\hbar\omega \geq 10.4$ eV.

If one assumes that the optically excited electrons are not inelastically scattered, the energy distribution curve can be expressed by Eq. (1).[1]

$$N(E) = CT(E)N_C(E)N_V(E-\hbar\omega). \qquad (1)$$

Here, $N(E)$ is the energy distribution of photoemitted electrons, $C$ is a constant, $T(E)$ is the probability for escape of an electron excited to final state of energy $E$, $N_C$ is the conduction-band optical density of states, and $N_V$ is the valence-band optical density of states. The method of analysis allows the separation of the factor $N_V(E-\hbar\omega)$ from the factor $T(E)N_C(E)$; thus, it is possible to determine whether the low-energy peak in Fig. 6 is fully uncovered. The valence-band optical density of states was derived from each of several pair of EDC's. The results of these different calculations were essentially identical, and $N_V$ so derived is shown in Fig. 7. This analysis indicates peaks in $N_V$ at 0.4, 2.4, and 5.5 eV below the Fermi level.

[13] C. N. Berglund and W. E. Spicer, Phys. Rev. **136**, A1030 (1964).

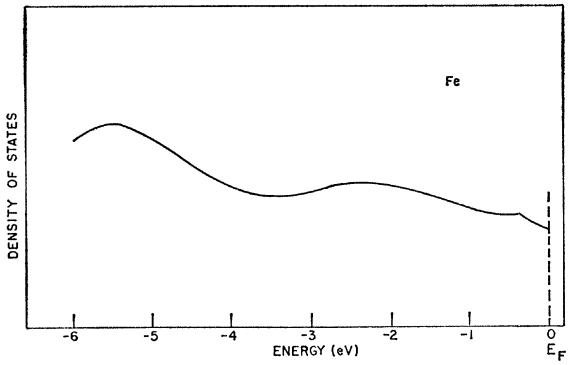


FIG. 7. Valence-band optical density of states in iron.

Inelastic scattering can affect EDC's by smoothing structure and can cause shifting of peaks to lower energies.[13] Although no strong scattering effects are observed in these Fe data (see below), it is likely that some inelastic scattering does occur. For this reason, the actual structure in the Fe density of states may be stronger than shown in Fig. 7, and the peaks may lie at slightly higher energies than indicated above.

The product $T(E)N_C(E)$ was also obtained from the Fe data by using Eq. (1). It is shown in Fig. 8. This analysis confirmed the earlier observation that $N_C$ is essentially constant above the threshold region —i.e., $6.0 \leq (E-E_F) \leq 11.6$ eV.

In order to check the model used in this analysis (i.e., that the optical transition probability depends only on the initial and final densities of states) and to verify the optical density of states obtained by this model, EDC's covering the experimental range of photon energy were calculated by using the curves shown in Figs. 7 and 8 and Eq. (1). Results of these calculations are shown superimposed on the experi-

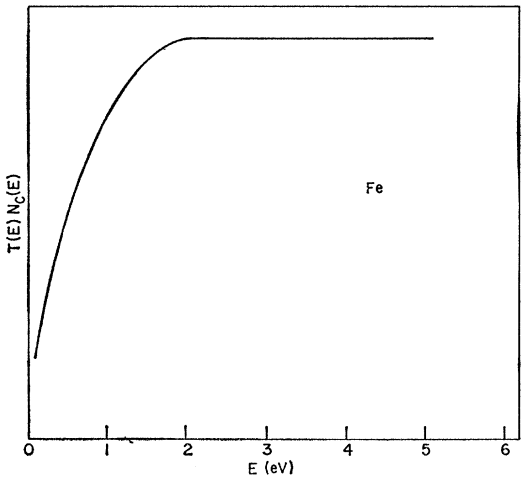


FIG. 8. Product $T(E)N_C(E)$ for iron (without Cs).

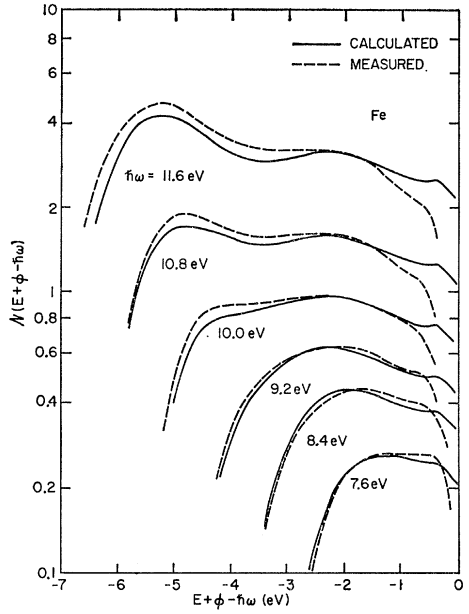


FIG. 9. Calculated and measured energy distributions of photoemitted electrons from iron.

mental curves in Fig. 9. The calculated curves have been fitted to the experimental curves at one point. In general, the agreement between the two sets is good. At higher values of photon energy, the measured EDC's are found to have fewer high-energy and more low-energy electrons than the calculations predict. This behavior is believed to be due to inelastic scattering.[13] The curves in Fig. 9 indicate that scattering effects are observable in the EDC's, but that these effects are not dominant.

## V. PHOTOEMISSION FROM IRON WITH A MONOLAYER OF CESIUM

### A. Quantum Yield

The quantum yield of Fe with approximately one monolayer of Cs on its surface is shown in Fig. 10.

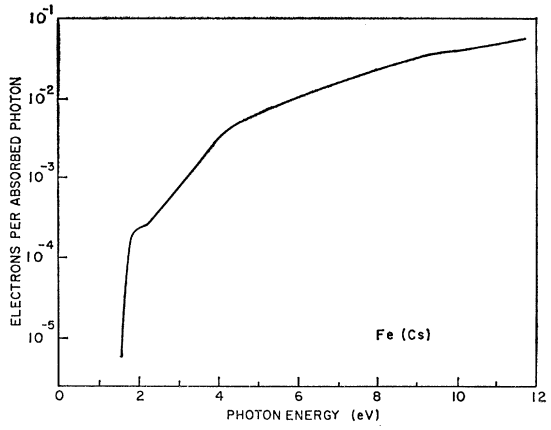


FIG. 10. Quantum yield for iron (with Cs).

(These data have been corrected for the transmission of the LiF window and the reflectance of Fe.) A well-defined shoulder is observed near 2 eV in the yield curve. This structure, which occurs in an energy region where there are no instrumentation problems, was carefully checked and verified because of its importance in the analysis of the data.

Because of difficulty in instrumentation near 4 eV, the yield data in this region are not as reliable as those at lower energies.[14] Fortunately, the experimental uncertainties in the yield near 4 eV do not affect the analysis presented here.

The square root of the quantum yield near threshold is shown in Fig. 11. A work function of 1.55 eV was obtained from this analysis.[1]

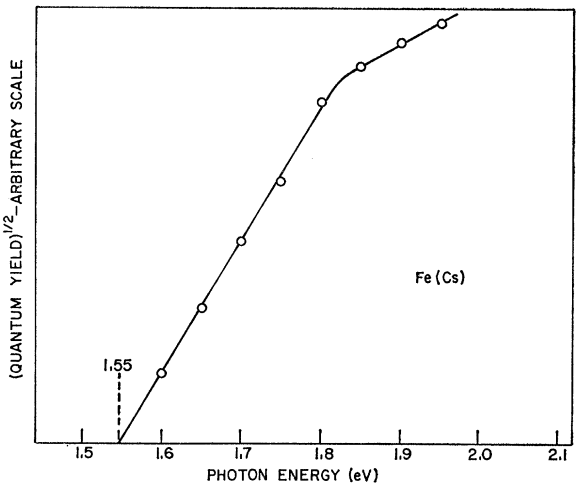


FIG. 11. Evaluation of the work function of iron (with Cs).

### B. Energy Distribution Curves

The EDC's from cesiated Fe are presented in Figs. 12–17. (All curves presented here have been normalized to the quantum yield. The scale used in these figures to indicate relative amplitudes from figure to figure is the same scale used in Figs. 4–6.) The EDC's for $2.0 \leq \hbar\omega \leq 2.8$ eV are plotted versus $E$ in Fig. 12(a) and versus $(E-\hbar\omega)$ in Fig. 12(b). The set of curves in Fig. 12(b) is of particular interest because of the strong transitions which occur at $(E-\hbar\omega) \approx -1.8$ eV, indicating an initial state approximately 0.3 eV below the Fermi level. The amplitude of this peak, and hence the strength of the transition, decreases rapidly as photon energy is increased. If corrections were made for $T(E)$, the change in the relative strength of this peak would be even more pronounced. The decrease in amplitude with increasing $\hbar\omega$ *cannot* be explained

[14] It is possible that the bolometer used to measure the intensity of the source for $\hbar\omega \leq 4.0$ eV reads low between 3.0 and 4.0 eV, thereby causing a false increase in yield.

in terms of a *rapid* decrease in the conduction-band density of states and constant momentum matrix elements, since such structure would also modify EDC's taken at higher photon energies, which other EDC's show is not the case. The strong transitions for $\hbar\omega \approx 2$ eV can only be explained by optical transitions for which the optical transition probability varies with $\hbar\omega$. This transition may be due to strong matrix elements between the density-of-states peak previously located

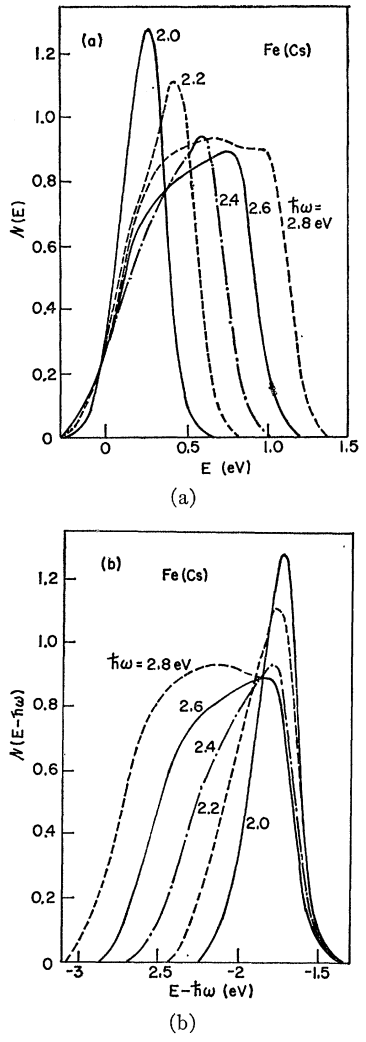


FIG. 12. Energy distributions of photoemitted electrons from iron (with Cs) for $\hbar\omega \leq 2.8$ eV; (a) plotted versus $E$; (b) plotted versus $E-\hbar\omega$.

0.4 eV below the Fermi level[15] and final states lying in the region near 1.7 eV above the Fermi level, or it may result from collective effects[16,17] such as those suggested in connection with the sharp peak which appears in the energy distributions from Ag for $\hbar\omega \approx 4$ eV.[8] It is

[15] The analysis in the previous section placed the peak 0.4 eV below the Fermi level, and these data place it 0.3 eV below the Fermi level; the difference is within the range of experimental error.

[16] J. J. Hopfield, Phys. Rev. **139**, A419 (1965).

[17] J. C. Phillips, Phys. Rev. **137**, A1835 (1965).

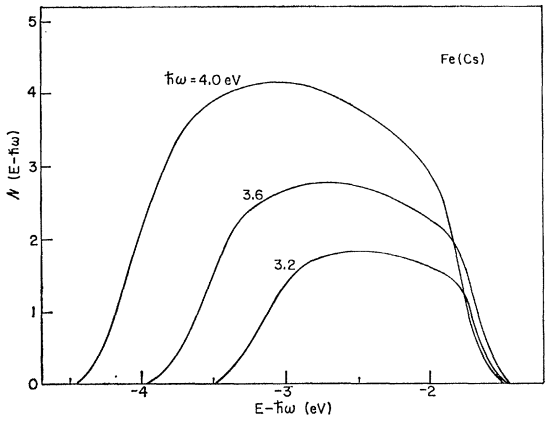


FIG. 13. Energy distributions of photoemitted electrons from iron (with Cs), plotted versus $E-\hbar\omega$, for $3.2 \leq \hbar\omega \leq 4.0$ eV.

the decreasing strength of these transitions (with increasing $\hbar\omega$) that causes the shoulder observed near 2 eV in the quantum yield (Fig. 10).

The EDC's taken at $\hbar\omega \geq 3.0$ eV are shown in Figs. 13–17. These EDC's differ from those obtained from Fe not coated with Cs (Figs. 4–6) in that they have a marked negative slope above the threshold region. This slope suggests that the conduction-band density of states decreases with increasing photon energy in this region and/or there is an increasing loss due to scattering at the higher energies. This interpretation is discussed in detail in Sec. V.C.

Except for the negative slope, the cesiated Fe data are consistent with noncesiated Fe results. In Sec. IV (noncesiated Fe), maxima were observed in the valence-band density of states at $(E-E_F)$ equal to $-0.4$, $-2.4$, and $-5.5$ eV. Since the work function of Fe with a monolayer of Cs is 1.55 eV, one would expect to find corresponding peaks in the EDC's at $(E-\hbar\omega)$

FIG. 14. Energy distributions of photoemitted electrons from iron (with Cs), plotted versus $E-\hbar\omega$, for $4.4 \leq \hbar\omega \leq 5.6$ eV.

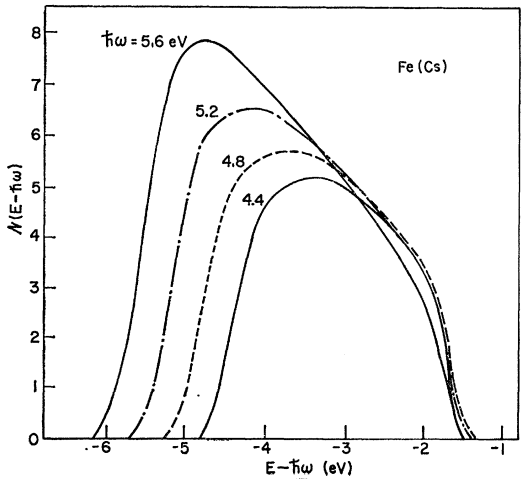

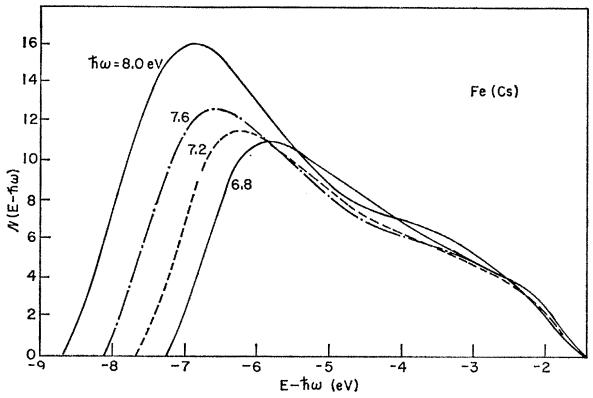


FIG. 15. Energy distributions of photoemitted electrons from iron (with Cs), plotted versus $E-\hbar\omega$, for $6.8 \leq \hbar\omega \leq 8.0$ eV.

to approximately equal $-1.9$, $-3.9$, and $-7.0$ eV. Indeed, a very strong peak is observed near $-1.9$ eV in Fig. 12(b), as noted above. This peak becomes smeared out and loses its identity as photon energy is increased (as the corresponding peak did in the noncesiated data). A broad shoulder is noted near $-3.9$ eV in Figs. 15–17. When the work function is taken into account, this corresponds to the broad peak at $-2.4$ eV in the valence-band optical density of states (Fig. 7). Similarly, structure is noted in Fig. 16 near $-7.0$ eV which corresponds to the peak at $-5.5$ eV in Fig. 7. Thus, although the structure is not as well defined in the cesiated Fe data, it is shown to be qualitative in agreement with the noncesiated Fe data. Similar results have been observed on cesiated and noncesiated Cu and Ag samples.[18]

In addition to the aforementioned structure in these EDC's, new structure is noted near $-8$ eV in Fig. 17. This structure appears to maintain a constant position

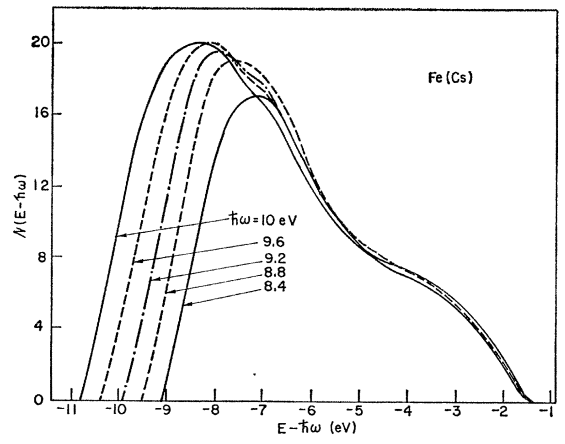


FIG. 16. Energy distributions of photoemitted electrons from iron (with Cs), plotted versus $E-\hbar\omega$ for $8.4 \leq \hbar\omega \leq 10.0$ eV.

[18] W. F. Krolikowski, Ph.D. dissertation, Stanford University, 1967 (unpublished).

on an $(E-\hbar\omega)$ plot, which suggests it may correspond to a peak in $N_V$ near $(E-E_F)=-6.5$ eV. However, the photon energy range over which this structure is observed is limited and the structure is neither strong nor well defined.

### C. Interpretation of the Data from Iron with a Monolayer of Cesium

The energy regions observed in the two sets of Fe data (with and without Cs) are compared schematically in Fig. 18. The zero of energy is taken at $E_F$ in this diagram. The high-energy limit on $N_C$ and the low-energy limit on $N_V$ are determined by the 11.6 eV cutoff of the LiF window. The low-energy portion of each crosshatched segment is rounded to indicate that

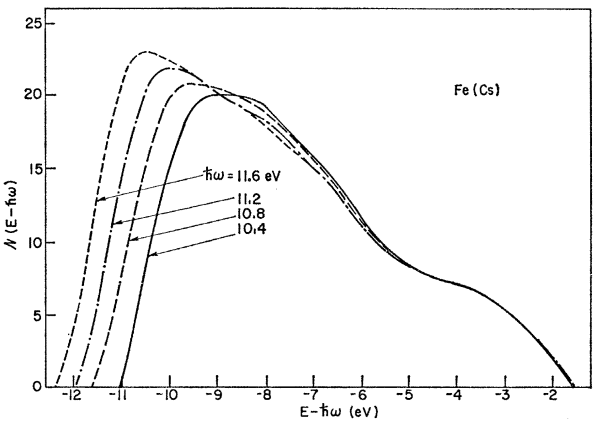


FIG. 17. Energy distributions of photoemitted electrons from iron (with Cs), plotted versus $E-\hbar\omega$, for $\hbar\omega \geq 10.4$ eV.

the analysis is complicated by the escape function $T(E)$ in these regions.

Although general agreement was shown between the two sets of data in the previous section, it was noted that the structure in the cesiated data is not as well defined as the corresponding structure in the noncesiated data. (The observed smearing of structure in the cesiated data could be due to increased electron-electron scattering and/or a reaction between the Fe and the Cs on the surface of the sample.) Thus, no new information is gained concerning the density of states in the regions previously uncovered in the noncesiated Fe data. However, the cesiated Fe data are useful in the regions exposed by reducing the work function. In particular, the reduction of $\phi$ allowed the observation of the strong transitions near $\hbar\omega=2$ eV, which were discussed in Sec. V.B.

A marked negative slope was observed in the EDC's presented in Sec. V.B. This slope could result from (1) a decreasing density of states in the region uncovered by lowering the work function, (2) strong electron-electron scattering, and/or (3) a reaction be-

tween the Cs and the Fe on the surface of the sample. However, several facts argue that the observed slope is due to a decreasing $N_C$.

Berglund and Spicer[13] have shown that electron-electron scattering will, in general, cause a reduction in the number of high-energy electrons in an EDC and an increase in the number of low-energy electrons. They have also shown that these effects increase markedly with photon energy. Obviously, these effects could cause a negative slope on an EDC. However, from Berglund and Spicer's results on Cu and Ag,[8] one would not expect strong scattering to cause these effects on EDC's taken at low photon energies. Further, one would expect the negative slope to increase rapidly with photon energy. An examination of the EDC's taken from cesiated Fe indicates that the slope above the threshold region stays relatively constant over a large range of photon energy. The fact that the normalized EDC's in Figs. 16 and 17 superimpose also argues against strong scattering effects.

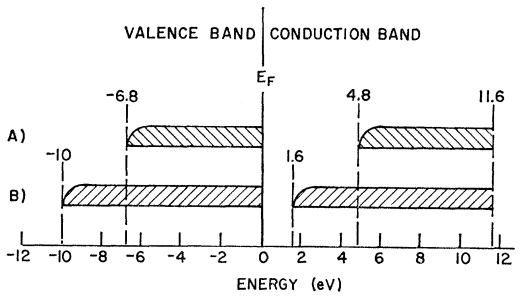


FIG. 18. Energy ranges of measurement for (a) Fe without Cs layer, and (b) Fe with Cs layer.

One might suggest that the observed negative slope is a result of the Cs. However, it is unlikely that Cs in small quantity would introduce any structure, particularly in this region of $N_C$. Detailed studies of Cu and Ag with and without a monolayer of Cs indicate that Cs can smear structure but that it does not introduce new structure.[18] Hence, it seems unlikely that scattering effects and Cs effects are sufficient to cause the observed slope.

Several pairs of EDC's were analyzed by the method described in Sec. IV.C to determine the conduction-band optical density of states in the region $(E-E_F)\leq 6.0$ eV. The results obtained from several pairs of EDC's were in close agreement, and the average result is shown in Fig. 19. This figure indicates that $N_C$ decreases by a factor of two in the region $2.5\leq(E-E_F)\leq 5.0$ eV. Consistent results were not obtained below this region, possibly because of the presence of transitions for which the momentum matrix elements are not equal. Since this analysis neglects all scattering and Cs effects, the factor of two is probably an upper limit on the decrease in $N_C$.

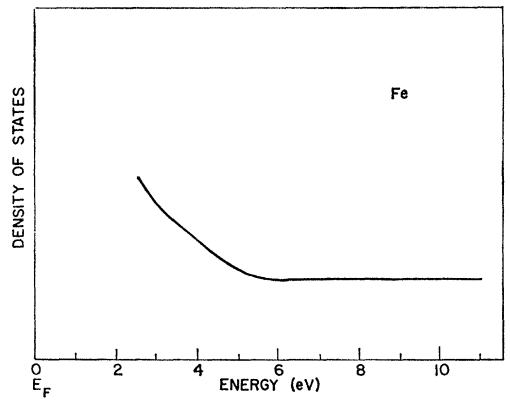


FIG. 19. Conduction-band optical density of states in iron as determined from iron coated with a monolayer of cesium.

## VI. DISCUSSION OF RESULTS

### A. Valence-Band Optical Density of States

In recent years several calculations have been made of the electronic band structure of Fe.[19–21] In general, the calculations show narrow, $d$-like bands within a few eV of $E_F$. These bands give rise to strong peaks in the valence-band density of states near $E_F$. These calculations are inconsistent with the valence-band optical density of states determined here from photoemission studies. The experimental results (Fig. 7) indicate that the "$d$-like bands" are very broad—greater than 6-eV wide—and that $N_V$ is void of strong structure in the region $-4\leq(E-E_F)\leq 0$ eV. Further, the calculations do not predict the large peak observed at $(E-E_F)=-5.5$ eV. Similar structure, not predicted by band calculations, was observed and reported earlier in Ni.[1]

The valence-band optical density of states in Fe as determined here is replotted in Fig. 20 with that re-

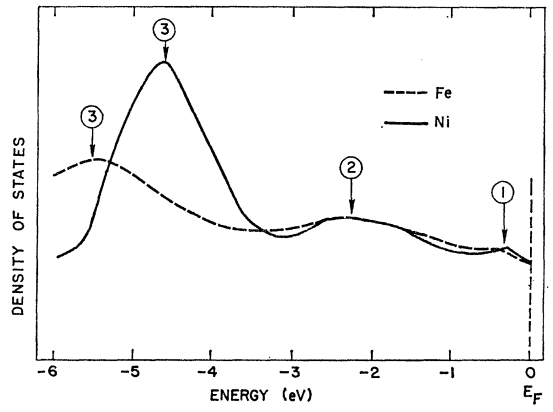


FIG. 20. Valence-band optical density of states in nickel (Ref. 1) and iron.

[19] J. Callaway, Phys. Rev. **99**, 500 (1955).
[20] L. F. Matthesis, Phys. Rev. **134**, A970 (1964).
[21] J. H. Wood, Phys. Rev. **126**, 517 (1962).

TABLE I. Position of structure in the optical densities of states in iron and nickel.

| Metal | Peak 1 (eV) | Peak 2 (eV) | Peak 3 (eV) |
|---|---|---|---|
| Fe | $-0.35\pm0.1$ | $-2.4\pm0.2$ | $-5.5\pm0.2$ |
| Ni | $-0.3\pm0.1$ | $-2.2\pm0.2$ | $-4.6\pm0.1$ |

ported in Ni.[1] The amplitude of the Fe curve relative to the Ni curve in Fig. 20 is arbitrary, since the relative densities of states are not known. The position in energy (relative to the Fermi level) of each peak labeled in Fig. 20 is given in Table I.

It is clear from Fig. 20 and Table I that the optical density of states of Fe is very similar to that of Ni in the region $-3.5\leq(E-E_F)\leq0$ eV. Further, both metals have a peak in $N_V$ below this region (i.e., peak 3). The low peak in Fe is not as strong as the corresponding peak in Ni, and it occurs at a lower energy.

The similarity between the Fe and the Ni results, particularly in the region $-3.5\leq(E-E_F)\leq0$ eV, suggests that crystal structure is relatively unimportant in the determination of $N_V$. Fe is bcc and Ni is fcc. The similarity does not, however, support the rigid-band model. The rigid-band model would predict similar structure in $N_V$ of Fe and Ni, but at different energies (relative to the Fermi level) since Fe has two less electrons than Ni. The similarity between Ni and Fe could be attributed to a common valence-band complex in these metals.[22] However, this and other models suggested in the literature are not sufficiently quantitative to allow direct comparison with the experimental results.

The strong low-energy peaks (peaks 3 in Fig. 20) observed in Ni and Fe are of particular interest because they are not predicted by band calculations. Since Fe and Ni are ferromagnetic, one can perturb the calculations by varying the exchange energy $\Delta E_d$ between the spin-up and the spin-down $d$ bands. However, in order to obtain bands from the calculations as wide as those observed in the photoemission results, one would have to postulate a $\Delta E_d$ in both Ni and Fe significantly larger than the values estimated from ferromagnetic properties ($\approx0.3$ eV for Ni; $\approx1.4$ eV for Fe).[23] Further, although large values of $\Delta E_d$ would result in broad bands, they would not give rise to peaks near $(E-E_F)=-5$ eV as strong as those observed in Fe and Ni.

Since the experimentally valence-band optical densities of states in Fe and Ni differ rather markedly from those derived from band calculations, it is suggested that conventional one-electron models do not adequately describe the electronic states in these metals as seen in the optical transitions and that many-body effects must be considered. Phillips[24] has suggested that the low-energy peak in Ni may result from a many-body resonance. It will be possible to examine this and other many-body models in more detail as experimental data become available on other transition metals.[25]

### B. Conduction-Band Optical Density of States

The data taken from Fe (without Cs) indicate that $N_C$ in Fe is approximately constant over the range $6.0\leq(E-E_F)\leq11.6$ eV. This result is consistent with the results reported on Ni,[1] Cu, and Ag.[8] The data taken from Fe with a monolayer of Cs on its surface suggest that $N_C$ decreases by approximately a factor of two in the region $2.5\leq(E-E_F)\leq5$ eV. This interpretation should be treated with caution, however, because a detailed, self-consistent analysis of the cesiated Fe data is not possible because of the presence of nonconstant matrix elements and the lack of a good quantitative description of electron-electron scattering in these data. A slow decrease in $N_C$ in Fe could be attributed to strong mixing of empty $s$, $p$, and $d$ bands.

The reflectance $R(\omega)$ (Fig. 1) can be used in conjunction with the photoemission results to suggest features in the conduction-band density of states in the region $0\leq(E-E_F)\leq2$ eV. The reflectance of Fe is replotted in Fig. 21 with that of Ni.[26] A detailed analysis of the Ni data[1] showed that the peak observed near 5 eV in $R(\omega)$ of Ni is due to transitions between peak 3 in $N_V$ of Ni (Fig. 20) and a relatively high density of empty $d$-like states just above the Fermi level. One observes a shoulder in $R(\omega)$ of Fe near 6 eV. Considering the Ni results and the relative size and

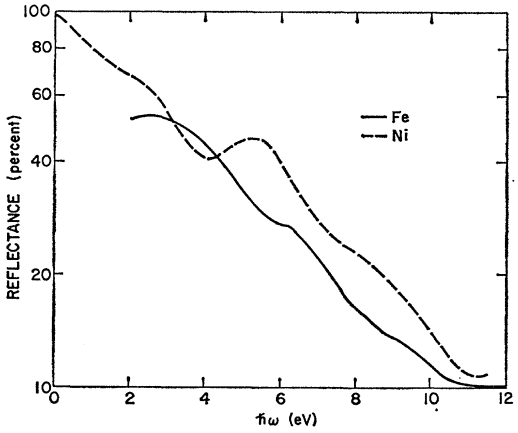


FIG. 21. Reflectance of nickel (Ref. 26) and iron.

[22] See, for example, L. Pauling, Proc. Natl. Acad. Sci. U.S. **39**, 551 (1953).

[23] E. P. Wohlfarth, in *Proceedings of the International Conference on Magnetism, Nottingham, 1964* (Institute of Physics and the Physical Society, London, 1965), pp. 51–54.

[24] J. C. Phillips, Phys. Rev. **140**, A1254 (1965).

[25] A. Y.-C. Yu and W. E. Spicer, Phys. Rev. Letters **17**, 1171 (1966).

[26] H. Ehrenreich, H. R. Philipp, and D. J. Olechna, Phys. Rev. **131**, 2469 (1963).

position of the low-energy peaks (peaks 3 in Fig. 20) in $N_V$ of Ni and Fe, it seems reasonable to assume that the shoulder near 6 eV in $R(\omega)$ of Fe is due to transitions from peak 3 to states just above the Fermi level. The relatively high density of states near $E_F$ so implied is not surprising since one would expect the density of states to be roughly continuous through the Fermi level.

It is not possible to derive a quantitative model for $N_C$ in Fe in the region $0 \leq (E-E_F) \leq 2.5$ eV because the optical conductivity is not well known over a wide range of photon energy and because transitions for which the momentum matrix elements are not constant occur near $\hbar\omega = 2$ eV. It is interesting to note the broad shoulder in $R(\omega)$ of Fe (Fig. 21) near 2 eV. It is likely that this shoulder results from the strong transitions observed in Sec. V.B for $\hbar\omega \approx 2$ eV.

## VII. CONCLUSIONS

The photoemission results indicate that conservation of wave vector **k** is not an important selection rule for the dominant optical transitions in Fe for the range of photon energy $6.0 \leq \hbar\omega \leq 11.6$ eV. Rather, it is found that these data can be interpreted in a consistent manner by assuming that the optical transition probabilities depend only on the initial and the final densities of states. Similar results have been reported on a number of metals, including Ni,[1] Gd,[27] Cu, and Ag.[8,28,29] This result indicates that the initial and the final states involved in the observed optical transitions cannot be described adequately in terms of Bloc one-electron wave functions. This behavior may be due to many-body effects associated with localization of the hole produced by the excitation[3] or to a variety of other many-body effects.

The results obtained at lower photon energies—$2 \leq \hbar\omega \leq 6$ eV—from Fe (coated with a monolayer of Cs to reduce the work function) also suggest that the optical transition probabilities depend only on the initial and the final densities of states (i.e., nondirect transitions). One notable exception is strong transitions observed near $\hbar\omega = 2$ eV for which the momentum matrix elements vary markedly with photon energy.

The fact that nondirect transitions (non-**k**-conserving and constant momentum matrix elements) dominate the EDC's observed from Fe (without Cs) allows the direct determination of the valence-band optical density of states in the region $-6.0 \leq (E-E_F) \leq 0$ eV and the conduction-band optical density of states in the region $5.5 \leq (E-E_F) \leq 11.6$ eV.

The valence-band optical density of states $N_V$ is found to be very broad and relatively constant over the range observed with maxima at $(E-E_F) = -0.35$, $-2.4$, and $-5.5$ eV. This experimental result differs markedly from band calculations which predict narrow $d$-like bands and strong peaks in $N_V$ near $E_F$. This result is further evidence that one-electron models do not adequately describe the electronic structure in Fe.

The $N_V$ determined in Fe is very similar to that previously obtained in Ni.[1] Both metals have a dominant, anomalous peak near $(E-E_F) = -5$ eV. The peak in Fe is not as strong and occurs at a lower energy than in Ni. These peaks are consistent with structure observed in the reflectance data of Fe and Ni. The similarity between Ni and Fe suggests that the energy distributions of electrons in the region observed in these two materials do not depend strongly upon crystal symmetry—Fe is bcc and Ni is fcc.

The conduction-band optical density of states $N_C$ in Fe is found to be approximately constant in the region $5.5 \leq (E-E_F) \leq 11.6$ eV. The data obtained from Fe with a reduced work function *suggest* that $N_C$ decreases by approximately a factor of two in the region $2.5 \leq (E-E_F) \leq 5.0$ eV.

In summary, several similarities have been found in the electronic structures of Fe and Ni. In particular, strong anomalous peaks are observed in $N_V$ of both metals near $(E-E_F) = -5$ eV. It appears that the observed structures cannot be interpreted in terms of one-electron models and that many-body effects must be considered. It is not clear, however, whether the similarities of Ni and Fe result because both are transition metals or because both are ferromagnetic. Experimental data on other transition metals, such as Co and Pd, will help resolve this question.[25]

## ACKNOWLEDGMENTS

The authors are indebted to J. C. Phillips, Frank Herman, and several members of the staff of Stanford University for many stimulating discussions and helpful suggestions in the course of this work. One of us (A.J.B.) is grateful to the International Business Machines Corporation for support received from an IBM Resident Fellowship. The authors would also like to thank Phil McKernan and Art Harmon for the fabrication of the experimental tubes.

[27] A. J. Blodgett, Jr., W. E. Spicer, and A. Y.-C. Yu, in *Optical Properties and Electronic Structure of Metals and Alloys*, edited by F. Abeles (North-Holland Publishing Company, Amsterdam, 1966), pp. 246–256.
[28] C. N. Berglund, in Ref. 27, pp. 285–295.
[29] W. E. Spicer, in Ref. 27, pp. 296–315.